MR imaging of spinal cord and vertebral body infarction.

W T Yuh, E E Marsh, 3rd, A K Wang, J W Russell, F Chiang, T M Koci and T J Ryals

AJNR Am J Neuroradiol 1992, 13 (1) 145-154
http://www.ajnr.org/content/13/1/145

MR Imaging of Spinal Cord and Vertebral Body Infarction

William T. C. Yuh,[1] E. Eugene Marsh, III[2] Angela K. Wang,[3] James W. Russell,[2] Francis Chiang,[4] Timothy M. Koci,[4] and Tony J. Ryals[1]

Purpose: To study the usefulness of MR in the evaluation of spinal cord infarctions and associated findings. **Materials and Methods:** MR examinations of 12 patients (10 men and two women) were reviewed retrospectively. Onset of symptoms of spinal cord ischemia was abrupt in all patients; MR was performed 8 hr to 4 months after onset. Contrast-enhanced MR was performed in four of the patients. **Results:** Abnormal MR findings of the spinal cord included abnormal cord signal (11 of 12), best demonstrated on T2-weighted images, and morphologic changes (cord enlargement during the acute phase in nine patients and cord atrophy during the chronic phase in two), best demonstrated on T1-weighted images. Vascular abnormalities (aortic) were detected by MR in four of the 12 patients. Three of these four patients also had abnormal bone marrow signal, predominantly in the anterior half (one) or in multiple areas near the endplate and/or deep medullary portion of the vertebral body involving several vertebrae (two). T1-weighted images were not sensitive in detecting signal changes in either the bone marrow (two of three) or spinal cord (nine of 12). Enhanced MR imaging was performed in four patients (two in the acute phase and two in the chronic phase) and showed diffuse enhancement of the spinal cord proximal to a relatively unenhancing distal conus in one of the two patients imaged during the acute phase. No abnormal enhancement was noted in the other three patients. **Conclusion:** MR is a useful means of detecting spinal cord infarction and associated vascular and bony changes. The patterns of bone marrow abnormalities reflect the underlying pathophysiology of the blood supply to the spinal cord and bone. The associated vascular and bone marrow abnormalities serve as additional information for the diagnosis of spinal cord infarction.

Index terms: Spinal cord, infarction; Spinal cord, magnetic resonance

AJNR 13:145–154, January/February 1992

Although there are no good epidemiologic data on the prevalence of spinal cord infarctions, they are generally considered to be rare (1–9). Some investigators think they occur more frequently than is commonly reported (5, 6). Ischemic spinal cord infarctions are difficult clinical diagnoses. In the past, radiologic diagnosis has been considered a diagnosis of exclusion. Myelography and computed tomography (CT) can help identify cord swelling, but these techniques are limited in their ability to visualize internal cord structure. In 1971, Di Chiro (7) reported the value of selective spinal cord angiography in improving recognition of occlusive vascular disease affecting the spinal cord. MR has proved to be a valuable noninvasive way to evaluate spinal cord disease. This article discusses the magnetic resonance (MR) findings associated with spinal cord and vertebral body infarctions and reviews the literature.

Received July 3, 1990; accepted and revision requested October 22, 1990; revision received June 4, 1991; final acceptance, June 6.

Presented at 28th Annual Meeting of the ASNR, Los Angeles, CA, March, 1990.

[1] Department of Radiology, The University of Iowa College of Medicine, Iowa City, IA 52242. Address reprint requests to W.T.C. Yuh.

[2] Department of Neurology, The University of Iowa College of Medicine, Iowa City, IA 52242.

[3] Department of Radiology, Rancho Los Amigos Medical Center, Downey, CA 90942.

[4] Department of Radiology, Harbor-University of California, Los Angeles, Medical Center, Torrance, CA 90509.

AJNR 13:145–154, Jan/Feb 1992 0195-6108/92/1301-0145

Materials and Methods

MR examinations of 12 patients with a clinical diagnosis of spinal cord infarction were reviewed retrospectively. There were 10 men and two women 17–85 years old (mean, 56 years). All patients had abrupt onset of symptoms of spinal cord ischemia.

All MR examinations were performed from 8 hr to 4 months after the onset of symptoms. Eleven patients were

TABLE 1: Summary of Patients with Spinal Cord Infarctions

Case No.	Age	Sex	Location	Possible Cause	Interval to Onset of Symptoms	Interval to MR	Cord Size	T1 Signal	T2 Signal	Vascular Abnormalities	Bone Marrow Abnormalities
1	76	M	Thoracolumbar	Aortoiliac bypass	Immediately after surgery	8 hr	Enlarged	No change or isointense	Increased	Yes	Yes
2	64	M	Thoracolumbar	DeBakey III dissection	1 hr	48 hr	Enlarged	No change or isointense	Increased	Yes	Yes
3	69	M	Thoracolumbar	Aortofemoral bypass	Immediately after surgery	10 hr[a]	Unable to evaluate	Unable to evaluate	Unable to evaluate	Yes	Yes
4	85	F	Thoracolumbar	Femoroiliac bypass	Immediately after surgery	24 hr	Enlarged	No change or isointense	Increased	Yes	No
5	75	M	Thoracolumbar	Subarachnoid bleeding	3 hr	19 hr	Enlarged	No change or isointense	Increased	No	No
6	60	F	Cervical	Hypotension	12 hr	16 hr	Enlarged	No change or isointense	Increased	No	No
7	27	M	Cervical	Strangling	2 hr	4 mo	Reduced	No change or isointense	Increased	No	No
8	68	M	Thoracolumbar	Unknown	Unable to evaluate	48 hr	Enlarged	Decreased	Increased	No	No
9	17	M	Thoracolumbar	Hypotension	Immediate	48 hr	Enlarged	No change or isointense	Increased	No	No
10	50	M	Thoracolumbar	Unknown	Unable to evaluate	4 mo	Reduced	Decreased	Increased	No	No
11	42	M	C5, T2	Acute disk herniation	Immediate	4 da	Enlarged	Decreased	Increased	No	No
12	39	M	T6–T8	Unknown	Unable to evaluate	2 da	Enlarged	No change or isointense	Increased	No	No

[a] Inadequate coil position.

examined with a 0.5-T scanner and one was examined with a 1.5-T superconductive scanner. All patients had 0.3- to 0.5-cm parasagittal T1-weighted, 350–450/20 (TR/TE), and T2-weighted, 1700–2000/80–100, images with vertical phase encoding. Gradient-moment nulling was used on all T2-weighted pulse sequences; no gradient-echo technique was performed. Additional axial T1- and/or T2-weighted images with 0.5- to 1-cm thickness were obtained in other planes depending on the individual case. Contrast-enhanced MR imaging was performed in four patients immediately after IV injection of 0.1 mmol/kg of gadopentetate dimeglumine.

Results

Clinical information and MR findings are summarized in Table 1. All 12 patients had a diagnosis of spinal cord infarction, either by clinical judgment (11) or angiography (one) (Figs. 1–4). A possible cause of infarction was identified in nine of the 12 patients: vascular surgery (three), aortic dissection (one), subarachnoid bleeding (one), hypotension (two), strangling (one), and acute disk herniation (one). Three patients had acute spinal cord infarctions without any known precipitating factors. Only one patient (from among the three without any known cause) (case 8) had an angiogram that showed an occluded right lumbar artery (L2). The diagnoses in the other 11 patients were based on clinical presentation and physical examination. All patients had clinical follow-ups of 2 months to 1 year. In four of the 12 patients, only minor improvement was seen in the neurologic deficits.

Abnormal findings were seen on MR images of the spinal cord in 11 of 12 patients. These included high signal intensity of the cord on the T2-weighted image in 11 of 12 patients and enlargement of the cord on the T1-weighted image in nine (Figs. 1, 2, and 4). In two patients without cord enlargement, MR studies performed 4 months after the onset of symptoms showed an atrophic cord with abnormal T2 signal. In only three of the 12 patients was abnormal cord signal seen on the T1-weighted image. Abnormalities in neural structures could not be evaluated by MR imaging in one patient because of the relatively low position of the lumbar coil (case 3) (Fig. 3). However, the absence of flow-void phenomena in the distal aorta due to complete occlusion and abnormal bone marrow signal on the T2-weighted image, located predominantly in the anterior portion of the vertebral body, were demonstrated in this patient. These findings support the clinical

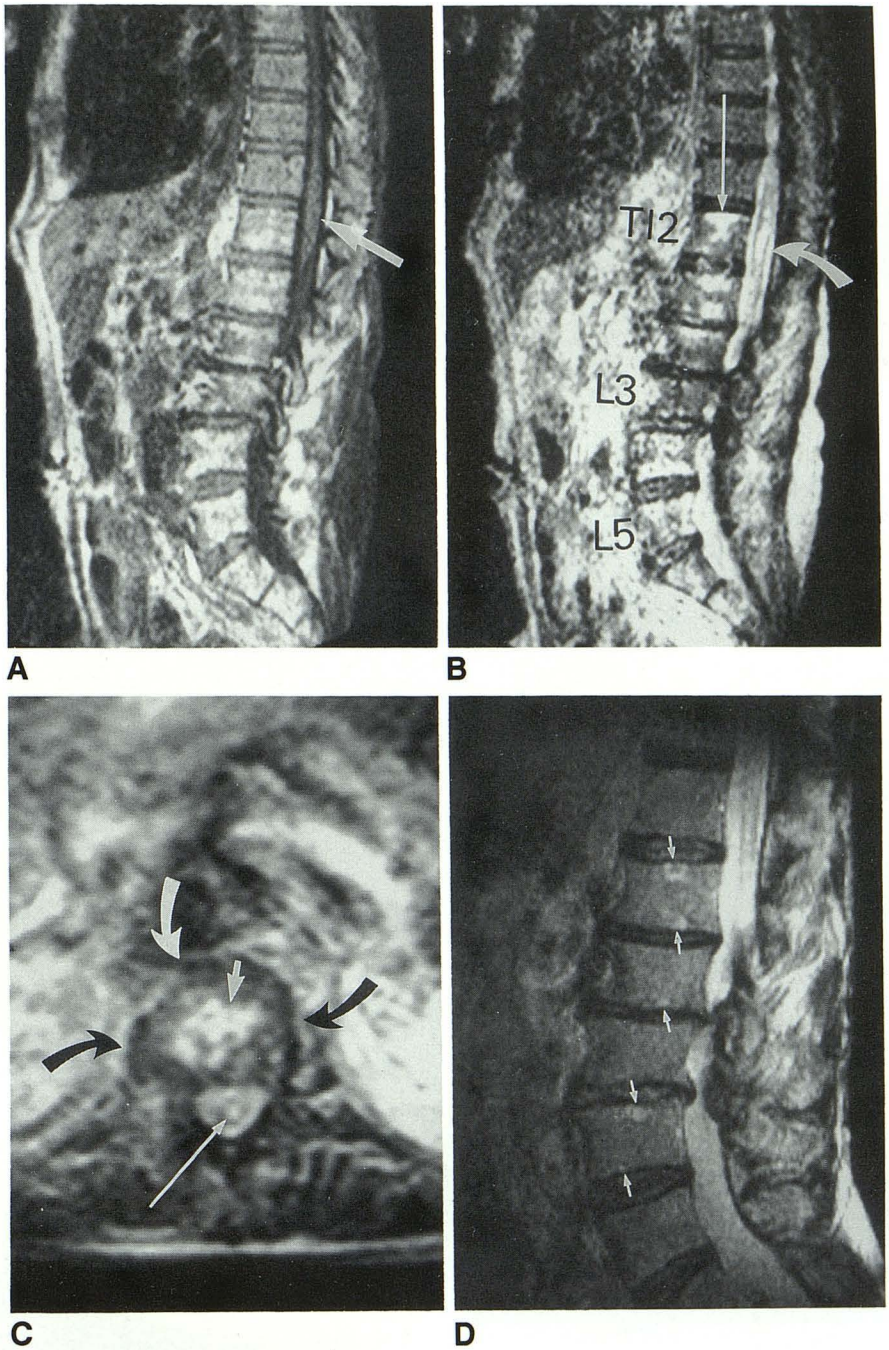

Fig. 1. Case 1: 76-year-old man had weakness of both lower limbs and T7 sensory deficit immediately after bilateral aortoiliac bypass for abdominal aortic aneurysm.

A, Parasagittal T1-weighted image (350/20) shows enlargement (*arrow*) of spinal cord.

B, Parasagittal T2-weighted image (2000/100) shows abnormal signal (*curved arrow*) within spinal cord from T11–L1 levels to conus. Abnormal bone marrow signal is also noted involving multiple vertebrae, especially T12–L1 levels, predominantly in areas near endplate and deep medullary portion of vertebral body. Characteristic triangular ischemic areas (*straight arrow*) correspond to regions most vulnerable to ischemia. Other possibly involved vertebrae include L4, L5, and S1. Flow-void phenomena of abdominal aorta are not seen on parasagittal images because of complete aortic occlusion. Bone marrow abnormalities are not obvious on T1-weighted image (*A*).

C, Axial T2-weighted image obtained at pedicle level shows abnormal signal in central gray matter of spinal cord (*long straight arrow*). Abnormal bone marrow signal shows location of ischemia in deep medullary portion (*short straight arrow*) of vertebral body (*curved arrows*).

D, Parasagittal T2-weighted image (2000/100) obtained with a surface coil 1 year later shows similar findings. However, these lesions (*arrows*) are much smaller, and triangular area in most vulnerable region now may represent true infarcted rather than ischemic areas.

diagnosis of spinal cord infarction caused by acute aortic occlusion.

Vascular abnormalities (aortic) were detected in four of the 12 patients. These included complete aortic occlusion (cases 1 and 3), DeBakey III aortic dissection (case 2), and saccular aneurysm with intraluminal clots (case 4). In three of these four patients, vascular abnormalities were first detected by MR. Abnormal bone marrow signal was seen in these three patients also and was demonstrated best on the T2-weighted image (Figs. 1–3). One of the three patients had a lesion involving predominantly the anterior half of one vertebral body (Fig. 3), whereas the other two had multiple bone marrow lesions located near the endplate and/or deep medullary portions of several vertebrae (Figs. 1 and 2). Abnormal bone marrow was demonstrated on the T1-weighted image (Fig. 3) in only one of the three patients in whom abnormal bone marrow was apparent on the T2-weighted image. One patient had a 1-year follow-up MR study that demonstrated persistence of bone marrow findings with a reduction in lesion size and a typical triangular configuration

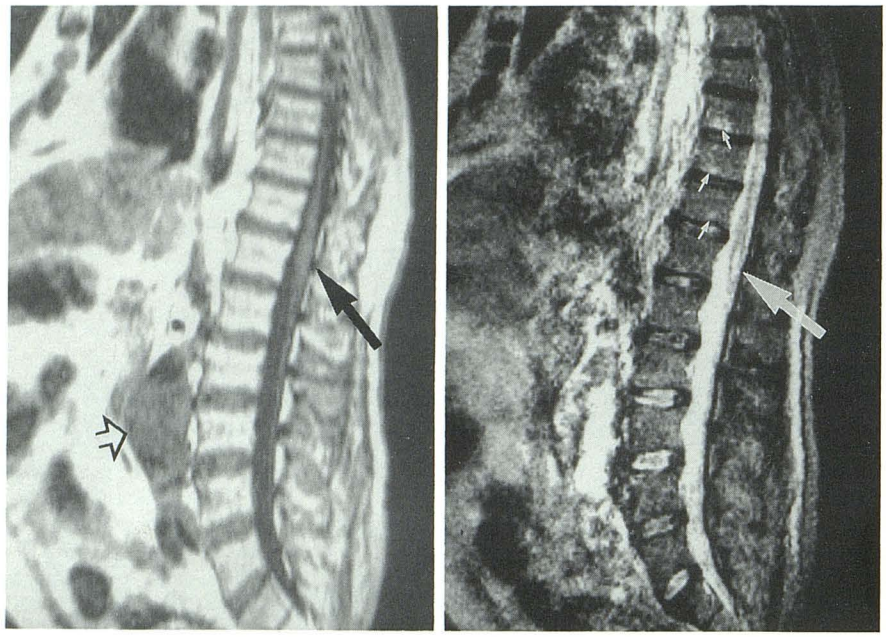

Fig. 2. Case 2: 64-year-old man had acute onset of chest pain due to DeBakey III dissecting aneurysm from aortic root to aortic bifurcation. He also had tingling of lower limbs progressing to paresthesia and eventually paralysis.

A, T1-weighted image (400/20) shows enlargement (*solid arrow*) of spinal cord near conus. Partially occluded abdominal aortic aneurysm (*open arrow*) is noted also.

B, T2-weighted image (2000/100) corresponding to *A* shows abnormal signal within conus (*large arrow*). Multiple areas of abnormal bone marrow signal (*small arrows*) involving lower thoracic vertebrae near endplate and watershed zone are shown.

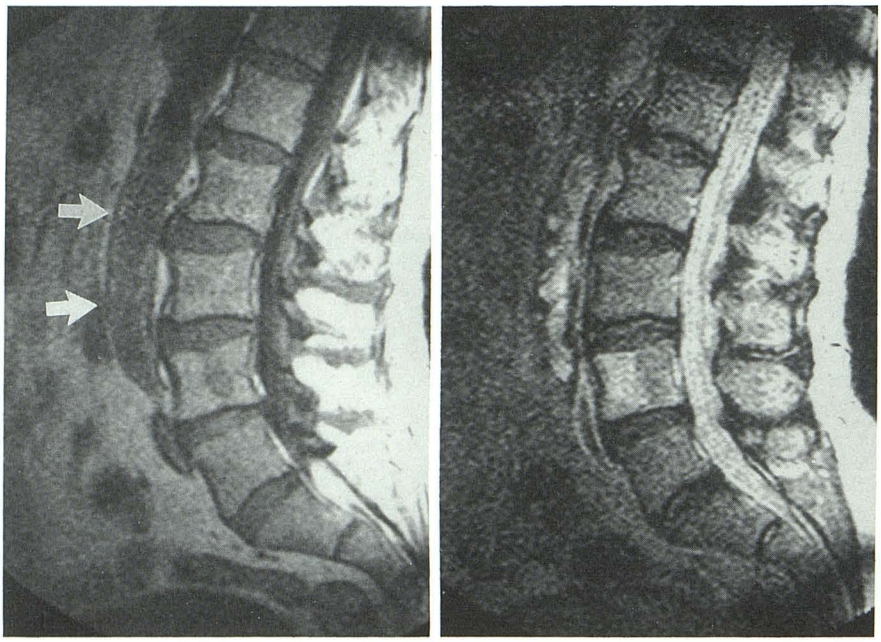

Fig. 3. Case 3: 69-year-old man initially had acute onset of back pain and numbness of left lower limb. Eighteen days after left axillary–bifemoral bypass, he again had acute onset of back pain, paresthesia of lower limbs progressing to paralysis, and elevated levels of blood urea nitrogen and creatinine. Clinically, he was diagnosed as having a spinal cord and cauda equina infarction.

A and *B*, Parasagittal T1-weighted (416/20) (*A*) and T2-weighted (1700/100) (*B*) images show completely occluded distal abdominal aorta (*arrows*) and abnormal bone marrow signal at L4 vertebra. Abnormal bone marrow signal was most prominent in anterior half of L4 vertebra, best seen on T2-weighted image. Low-signal area of L4 vertebra seen on T1-weighted image (*A*) most likely represents ischemic changes of deep medullary portion of vertebral body. Visualization of spinal cord at thoracolumbar junction is limited because of relatively low position of surface coil.

located both near the endplate and in the deep medullary portion of the vertebral body (Fig. 1D). These triangular areas may be the most vulnerable regions of the vertebral body during ischemia and may represent the true infarcted area.

Contrast-enhanced MR images were obtained in four of the 12 patients, two patients in the early phase of ischemia and two in the chronic phase. Only one of the two patients in the early phase showed diffuse enhancement of the spinal cord proximal to a sharply delineated, unenhancing distal conus. No significant abnormal enhancement was noted in the other three patients (one early phase, two chronic phase).

Discussion

Thirty-one pairs of segmental arteries and their regional equivalents supply the entire spinal column and surrounding structures including muscle, bone, and neural derivatives (1–19). In most cases, all these tissues at each level, with the exception of the spinal cord territory, receive their major blood supply from the two (one on each

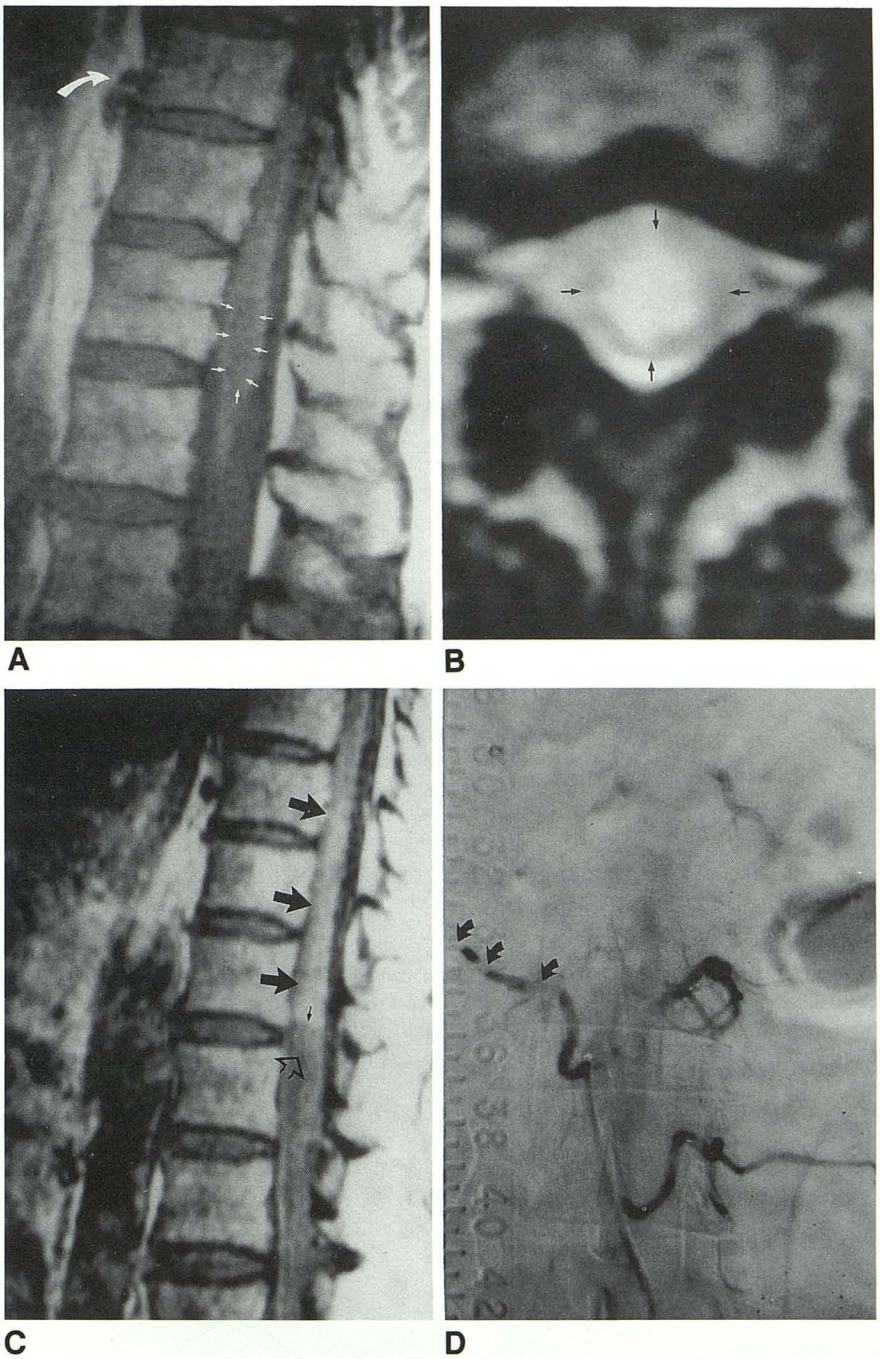

Fig. 4. Case 8: 68-year-old previously healthy man had acute onset of paresthesia progressing to paralysis of both lower limbs within 2 hr.

A, Parasagittal T1-weighted image (350/20) obtained 48 hr after onset of symptoms shows enlargement and decreased signal (*straight arrows*) of distal spinal cord. Note that renal artery (*curved arrow*) and inferior border of conus are slightly lower than disk level.

B, Axial T2-weighted image (2000/80) obtained through conus shows abnormal cord signal (*arrows*) involving predominantly gray matter.

C, Enhanced parasagittal T1-weighted image corresponding to *A* shows diffuse abnormal enhancement of distal spinal cord (*large solid arrows*) above disk level and unenhancing distal conus (*open arrow*) below disk level, which may represent true infarcted area. Note relatively linear cutoff (*small arrow*) between enhancing proximal and unenhancing distal conus just above disk level.

D, Lumbar arteriogram shows occluded right L2 segmental artery (*arrows*).

side) segmental arteries or their equivalents at the same and/or adjacent level (7, 8, 10, 17–19) (Figs. 5–7). Branches of the segmental arteries or their equivalents course dorsally and further divide into extraspinal branch arteries to supply muscle, bone, and nerve roots and intraspinal branch arteries (radicular arteries) to supply bone and neural structures including the spinal cord, dural meninges, and epidural structures (8, 10, 17–19) (Fig. 6). The radicular arteries are the first branches of the dorsal division of the segmental arteries or their regional equivalents. They enter the intervertebral foramina as either a single vessel or a number of vessels accompanying the emerging veins and spinal nerves. After entering the spinal canal, these paired radicular arteries on each side of the vertebrae may ultimately divide into a triad of vessels: the posterior central and prelaminar arteries to supply primarily the bone and, inconsistently, a radiculomedullary artery (medullary feeder) to supply primarily the spinal artery of the spinal cord (7, 8, 10, 17–19) (Figs. 5 and 6).

Unlike the paired posterior central and prelaminar arteries, the radiculomedullary artery may occur on only one side and does not always occur

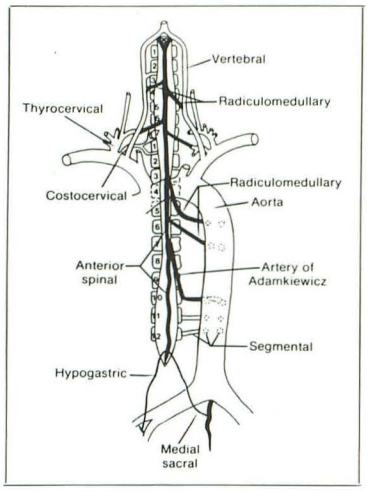

Fig. 5. Anterior view of blood supply to spinal cord from medulla to conus medullaris. Anterior spinal artery and its medullary feeders or radiculomedullary arteries are shown as a *heavy solid line*. Radiculomedullary artery is frequently unilateral and does not always occur at every vertebral level. Note obligatory cranially ascending course of radiculomedullary artery [7, 8, 10, 17].

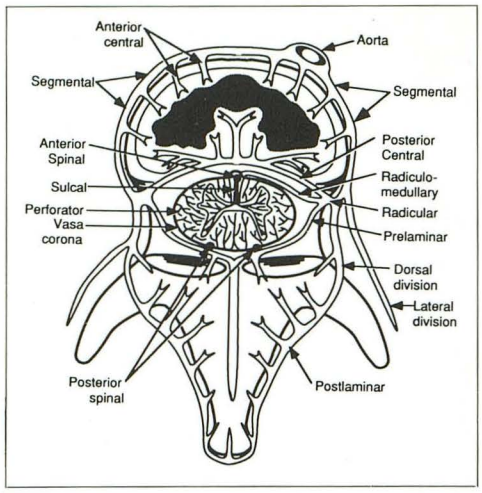

Fig. 6. Axial view of blood supply to bony vertebrae and spinal cord. Paired radicular arteries, derived from paired segmental arteries at each vertebral level, pass through intervertebral foramen and give rise to pairs of postcentral and prelaminar arteries and, occasionally, a unilateral radiculomedullary artery (triad). Anterior spinal artery gives rise to sulcal arteries that pass posteriorly through anterior median fissure to supply anterior two thirds of spinal cord. The two posterior spinal arteries give rise to posterior perforators that supply posterior one third of spinal cord, including dorsal column and posterior horns. Anterior and posterior spinal arteries are connected by vasa corona, which give off circumferential branches that supply lateral columns. Vertebral body is supplied mainly by anterior and posterior central arteries, whereas posterior element is supplied by pre- and postlaminar arteries. Posterior central arteries converge near center at posterior aspect of vertebral body and give rise to branches that supply central and posterior aspects of vertebral body. Anterior central arteries arise directly from segmental arteries and supply anterior and lateral portions of vertebral body. *Black area* is watershed zone (deep medullary portion) between anterior and posterior central arteries [8, 10, 17–19].

at each level. Radicular arteries have an obligatory ascending course since they always follow the nerve roots with increasing obliquity from the cranial to caudal levels (8, 10, 17). Therefore, the levels of spinal cord involvement are frequently not the same as those of the bone marrow, as seen in our patients (Fig. 5). In summary, the vertebral body is supplied mainly by the terminal branches (anterior central artery) derived from the paired segmental arteries at the same level and the posterior central artery derived from the paired radicular arteries at two adjacent levels (Figs. 6 and 7). The blood supply of the spinal cord comes from a limited number of medullary feeders that are derived from a segmental artery or its equivalent at a more caudal level (Figs. 5 and 6).

The blood supply to the entire spinal cord is dependent mainly on three longitudinal arterial trunks: a single anterior spinal artery and paired posterior spinal arteries. These spinal arteries extend from the medulla oblongata to the conus medullaris (1, 4, 7–17) (Fig. 5). Although these longitudinal trunks are usually continuous, the anterior spinal artery is narrowest in the midthoracic region and widest in the cervical region (9). The number of anterior radiculomedullary arteries supplying the anterior spinal artery rarely exceeds nine but ranges from two to 17. The artery of Adamkiewicz is the largest anterior medullary feeder and supplies the thoracolumbar region (Fig. 5). It occurs on the left side in 80% of

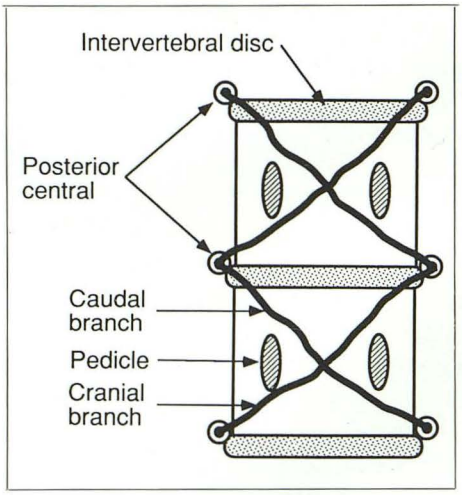

Fig. 7. Posterior view of blood supply to vertebral body. Posterior central arteries further divide into cranial and caudal branches, which supply two adjacent vertebrae. There are, therefore, four diagonal arteries, two from each side, converging centrally to supply posterior half of vertebral body [17–19].

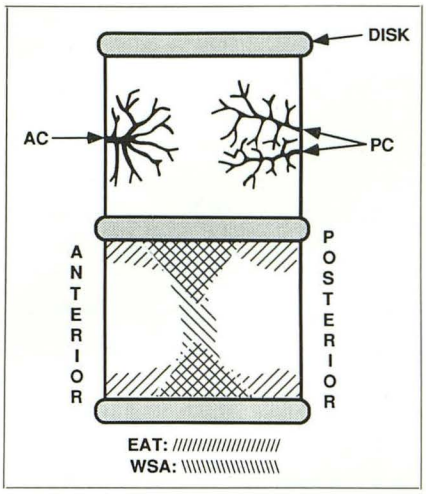

Fig. 8. Midparasagittal view of two adjacent vertebral bodies. Upper vertebra shows vascular territories of anterior central (AC) and posterior central (PC) arteries. Lower vertebra shows watershed area (WSA) in deep medullary portion and end arterial territory (EAT) near endplate. *Cross-hatched areas* have a triangular configuration located within both EAT and WSA and may represent areas more vulnerable to ischemia.

subjects and can arise anywhere between the T5 and L4 levels (T9–L2 in 85%, T9–T11 in 75%, L1–L2 in 10%, and T5–T8 in 15%) (9).

The posterior medullary feeders (radiculomedullary arteries) supplying the posterior spinal artery are more numerous, usually ranging from 10 to 23 (20, 21). The posterior spinal arteries are also supplied by radicular arteries derived from segmental arteries or their regional equivalents (including vertebral arteries and posterior inferior cerebellar arteries). In most cases, the artery of Adamkiewicz supplies the entire lumbosacral cord, including the posterior spinal arteries.

Because of the limited but critical sources of blood supply to the spinal cord, any pathologic processes that interfere with this crucial blood supply may result in ischemia and/or infarction in the spinal cord (1, 3–7, 11, 17–19, 22–36). Most spinal cord infarctions occur at the upper thoracic region or thoracolumbar junction. Infarctions in the latter site may result from occlusion of the artery of Adamkiewicz, which is frequently the only blood supply to the thoracolumbar junction (11, 17). In the upper thoracic regions, medullary feeder arteries are sparse, the anterior spinal artery is narrow, sulcus arteries are fewer and smaller, the spinal canal is narrow, and the spinal cord is in a watershed area between major feeding arteries (1, 8, 9). The vertical extent of spinal cord infarction may have from one to 15 segments, depending on the vascular anatomy of the cord and extent of occlusion. Single segmental infarction is frequently caused by ischemia in the watershed area, as occurs in hypotension (17). Single segmental infarction may also be seen in diseases that affect the small end arteries, such as emboli or focal vasculopathies. All of our patients with bone marrow abnormalities had vertical cord involvement involving several levels, probably caused by a more extensive disease of the aorta.

Although abnormal spinal cord signals were clearly demonstrated in most of our patients, the earliest MR image was obtained 8 hr after onset. Therefore, the earliest time that abnormal findings can be detected by MR remains to be determined. Only four of our patients had enhanced MR studies performed at various periods of cord ischemia. The efficacy of gadopentetate dimeglumine has yet to be determined, especially with regard to early detection and prognostic value. The cause of the sharp demarcation between the enhancing spinal cord and unenhancing distal conus is unknown (Fig. 4).

The prevalent distribution of abnormal bone marrow signal as seen in our limited number of cases has not been described previously. The recognition of abnormal bone marrow signal may be an important finding in establishing a vascular cause for an acute spinal cord syndrome. The blood supply of the bony spine includes anterior central, posterior central, prelaminar, and postlaminar branches (Fig. 6). The radicular arteries (intraspinal branch arteries) usually provide the greater part of the blood supply to the vertebral body (posterior central arteries) and arch (prelaminar arteries).

Anterior central arteries consist of many terminal branch vessels that come directly off the segmental arteries (Fig. 6). They penetrate the cortical bone of the vertebral body and supply the anterior and anterolateral portions. The central and posterior portions of the vertebral body are supplied mainly by four posterior central arteries. These arteries further divide into cranial and caudal branches, which supply two adjacent vertebral bodies (17–19) (Figs. 6 and 7). The cranial branches run upward and medially across the posterior surface of the vertebral body to enter a foramen near the center of the body. The caudal branches run downward and medially a similar distance toward the center of the body of the next distal vertebra. There are, therefore, four diagonal arteries, two from each side, converging centrally to enter the posterior surface to supply

the posterior and central portions of the vertebra (Fig. 7).

Because the central and posterior portions of the vertebral body receive their blood supply from multiple sources (Figs. 6 and 7) and the blood supply to the anterior and peripheral (near the endplate) portions of the vertebral body is mostly from end arteries (Figs. 6 and 8), it is not surprising that abnormal bone marrow signals were frequently seen near the endplate (Figs. 1B, 1D, and 2B) and deep medullary (watershed) (Figs. 1B, 1D, and 3A) or anterior (Fig. 3) portions of the vertebral body. A particular triangular area located within both the deep medullary portion and near the endplate may be more vulnerable to ischemia (Figs. 1B, 1D, 2B, and 8). Interestingly, a 1-year follow-up study in one patient showed a significant reduction in the size of the lesions. All these lesions were located within this vulnerable triangular region and probably represent the true infarcted areas (Fig. 1D). Although degenerative changes near the endplate have a high signal on the T2-weighted image and low signal on the T1-weighted image, they are usually presented as a linear lesion extending along the entire endplate. Involvement of the anterior half or the deep medullary portion of the vertebral body, especially in a triangular shape, is not typically seen in degenerative changes. Degenerative changes tend not to regress to the characteristic triangular shape (Figs. 1B and 1D). In addition, a central low signal with a peripheral high signal is a typical finding (Fig. 1D) in bone infarction of the femoral head, as reported previously. Most importantly, degenerative changes are seen most frequently in the lower lumbar spine (L4–L5 and L5–S1) and are seen infrequently at multiple levels in the higher lumbar or mid and lower levels of the thoracic spine.

All three patients with bone marrow abnormalities also had significant aortic disease (occlusion or dissection) that was readily demonstrated by MR. Because of the excellent collateral circulation among segmental arteries and their branches, a significant interruption of the blood supply to the anterior central and/or posterior central arteries must occur to cause ischemia within the vertebral body (Figs. 5–8). However, ischemia of a vertebral body is not always associated with a spinal cord infarction because the origin of the medullary feeder artery does not occur at each level and is frequently located more caudally. On the other hand, a single segmental artery occlusion may not always result in bone ischemia because of the excellent collateral circulation of the vertebral body (duplicate anterior central and quadruplicate posterior central arteries) (Fig. 4). Therefore, a wide disparity may exist between the level of spinal cord involvement and that of bone involvement, especially in patients who have a broad range of aortic disease with various degrees of occlusion at different vertebral levels.

The MR findings of avascular necrosis (AVN) in the region of the femoral head, hand, knee, and foot have been reported previously and typically show low signal intensity on T1-weighted images and high signal intensity on T2-weighted images (37–43). The MR appearance of vertebral body ischemia caused by aortic occlusion or dissection has not been described previously. This may be related to the difficult clinical and radiologic diagnoses in patients with acute aortic occlusion. There is only one report of MR findings of vertebral AVN, which was caused by recent trauma in five patients with radiologic evidence of compressed vertebrae containing an intravertebral vacuum cleft indicative of AVN (44).

All vertebral lesions in our patients demonstrated high signal intensity on T2-weighted images that was less obvious on T1-weighted images. In addition, a low-signal peripheral ring frequently seen in AVN was not seen in our limited number of cases during the acute phase. These are not characteristic MR findings of AVN involving the extraspinal bony structures, as reported previously (37–43). During the early phase of AVN, inflammatory cells, necrosis, and edema are the major components in the area of ischemia, whereas new bone formation and fibrosis predominate in the later phases (37, 38, 42, 44). Because these elements have different appearances on MR images, variability in the MR findings among patients and over time is to be expected, depending on which phase of AVN is present. All three patients with bone marrow abnormalities were imaged during a very early phase of ischemia (within first 48 hr), when necrosis, inflammation, and edema were predominant in the ischemic area without significant fibrosis and new bone formation. Therefore, our MR findings of bone ischemia are somewhat different from those of AVN in the extraspinal bone in that T2-weighted images were more sensitive than T1-weighted images and a peripheral low-signal ring was not seen during the acute phase of bone ischemia.

In conclusion, we found MR to be useful for detecting spinal cord infarction. Abnormal MR findings include abnormal signal of the spinal cord, best demonstrated on T2-weighted images, and changes in cord morphology (swelling or atrophy), best demonstrated on T1-weighted images. Other MR signs of ischemia include vascular or bone marrow abnormalities, which may serve as additional information to facilitate a correct diagnosis. The T1-weighted image is not as sensitive as the T2-weighted image in detecting cord signal changes or bone marrow abnormalities. The earliest time that MR can detect spinal cord infarction and the prognostic value of MR imaging with and without gadopentetate dimeglumine require further study.

Acknowledgments

We thank Daniel Loes, MD, and Yutaka Sato, MD, for reviewing the manuscript and Ronald Bergman, PhD, for assistance in the preparation of the anatomic drawings.

References

1. Sandson TA, Friedman JH. Spinal cord infarction: report of 8 cases and review of the literature. *Medicine (Baltimore)* 1989;68:282–292
2. O'Moore B. Anterior spinal artery syndrome. *Acta Neurol Scand* 1965;58:59–65
3. Rothman SM, Nelson JS. Spinal cord infarction in a patient with sickle cell anemia. *Neurology* 1980;30:1072–1076
4. Satran R. Spinal cord infarction. *Stroke* 1988;19:529–532
5. Albert ML, Greer WER, Kantowitz W. Paraplegia secondary to hypotension and cardiac arrest in a patient who has had previous thoracic surgery. *Neurology* 1969;19:915–918
6. Hughes JT, Brownell B. Spinal cord ischaemia due to arteriosclerosis. *Arch Neurol* 1966;15:189–202
7. Di Chiro G. Angiography of obstructive vascular disease of the spinal cord. *Radiology* 1971;100:607–614
8. Dommisse GF. The blood supply of the spinal cord. *J Bone Joint Surg [Br]* 1974;56B:225–235
9. El-Toraei I, Juler G. Ischemic myelopathy. *Angiology* 1979;30:81–94
10. Dommisse GF. The arteries, arterioles, and capillaries of the spinal cord. Surgical guidelines in the prevention of postoperative paraplegia. *Ann R Coll Surg Engl* 1980;62:369–376
11. Piscol K. *Blood supply of the spinal cord.* Berlin: Springer-Verlag, 1972
12. Doppman JL, Di Chiro G, Ommaya AK. *Selective arteriography of the spinal cord.* St. Louis, Warren H. Green, 1969
13. Gillilan L. The arterial supply of the human spinal cord. *J Comp Neurol* 1958;110:75–100
14. Turnbull IM. Blood supply of the spinal cord. In: Vinken PJ, Bruyn GN, eds. *Handbook of clinical neurology.* New York: Elsevier, 1972:478–491
15. Laguna J, Cravioto H. Spinal cord infarction secondary to occlusion of the anterior spinal artery. *Arch Neurol* 1973;28:134–136
16. Anderson NE, Willoughby EW. Infarction of the conus medullaris. *Ann Neurol* 1987;21:470–474
17. Lasjaunias P, Berenstein A. *Surgical neuroangiography. 3. Functional vascular anatomy of brain, spinal cord and spine.* Berlin: Springer-Verlag, 1990:40–55
18. Parke WW. Applied anatomy of the spine. In: Rothman RH, Simeone FA, eds. *The spine.* Philadelphia: WB Saunders, 1982:18–51
19. Willis TA. Nutrient arteries of the vertebral bodies. *J Bone Joint Surg [Am]* 1949;31-A:538–541
20. Hegedus K, Fekete I. Case report of infarction in the region of the posterior spinal arteries. *Eur Arch Psychiatry Neurol Sci* 1984;234:281–284
21. Hughes JT. Thrombosis of the posterior spinal arteries. A complication of an intrathecal injection of phenol. *Neurology* 1970;20:659–664
22. Spiller WG. Thrombosis of the cervical anterior median spinal artery; syphilitic acute anterior poliomyelitis. *J Nerv Ment Dis* 1909;36:601–613
23. Haft H, Finneson BE, Cramer H, Fiol R. Periarteritis nodosa as a source of subarachnoid hemorrhage and spinal cord compression. *J Neurosurg* 1957;14:608–616
24. Boden G. Radiation myelitis of the cervical spinal cord. *Br J Radiol* 1948;21:464–469
25. Reagan TJ, Thomas JE, Colby MY. Chronic progressive radiation myelopathy. *JAMA* 1968;203:128–132
26. Hughes JT, Brownell B. Cervical spondylosis complicated by anterior spinal artery thrombosis. *Neurology* 1964;14:1073–1075
27. Grinker RR, Guy CC. Sprain of cervical spine causing thrombosis of anterior spinal artery. *JAMA* 1927;88:1140–1142
28. Foo D, Rossier AB, Cochran TP. Complete sensory and motor recovery from anterior spinal artery syndrome after sprain of the cervical spine. *Eur Neurol* 1957;23:1119–1123
29. Welborn MB Jr, Sawyers JL. Acute abdominal aortic occlusion due to nonpenetrating trauma. *Am J Surg* 1969;118:112–116
30. Ikeda H, Ushio Y, Hayakawa T, Magami H. Edema and circulatory disturbance in the spinal cord compressed by epidural neoplasms in rabbits. *J Neurosurg* 1980;52:203–209
31. Blumbergs PC, Byrne E. Hypotensive central infarction of the spinal cord. *J Neurol Neurosurg Psychiatry* 1980;43:751–753
32. Rao KR, Donnenfeld H, Chusid JG, Valdez S. Acute myelopathy secondary to spinal venous thrombosis. *J Neurol Sci* 1982;56:107–113
33. Lyon LW. Transfemoral vertebral angiography as a cause of an anterior spinal artery syndrome. *J Neurosurg* 1971;35:328–330
34. Perry MO. The hemodynamics of temporary abdominal aortic occlusion. *Ann Surg* 1968;168:193–200
35. Brewer LA, Fosburg RG, Mulder CA, Verska JJ. Spinal cord complications following surgery for coarctation of the aorta. *J Thorac Cardiovasc Surg* 1972;64:368–381
36. Elliott JP, Szilogyi DE, Hageman JH, et al. Spinal cord ischemia: secondary to surgery of the abdominal aorta. In: Bernard VM, Towne JB, eds. *Complications in vascular surgery.* New York: Grune & Stratton, 1985:241–310
37. Coleman BG, Kressel HY, Dalinka MK, Scheibler ML, Burk DL, Cohen EK. Radiographically negative avascular necrosis: detection with MR imaging. *Radiology* 1988;168:525–528
38. Beltran J, Herman LJ, Burk JM, et al. Femoral head avascular necrosis. MR imaging with clinical-pathologic and radionuclide correlation. *Radiology* 1988;166:215–220

39. Mitchell DG, Rao VM, Dalinka MK, et al. Femoral head avascular necrosis: correlation of MR imaging, radiographic staging, radionuclide imaging, and clinical findings. *Radiology* 1987;162:709–715
40. Mitchell DG, Kressel HY, Arger PH, Dalinka M, Spritzer CE, Steinberg ME. Avascular necrosis of the femoral head: morphologic assessment by MR imaging with CT correlation. *Radiology* 1986;161:739–742
41. Reinus WR, Conway WF, Totty WG, et al. Carpal avascular necrosis: MR imaging. *Radiology* 1986;160:689–693
42. Björkengren AG, AlRowaih A, Lindstrand A, Wingstrand H, Thorngren K-G, Pettersson H. Spontaneous osteonecrosis of the knee: value of MR imaging in determining prognosis. *AJR* 1990;154:331–336
43. Sierra A, Potchen EJ, Moore J, Smith HG. High-field magnetic-resonance imaging: aseptic necrosis of the talus. A case report. *J Bone Joint Surg [Am]* 1986;68-A:927–928
44. Naul LG, Peet GJ, Maupin WB. Avascular necrosis of the vertebral body: MR imaging. *Radiology* 1989;172:219–222

Please see the Commentary by Mikulis on page 155 in this issue.